



IGC Newsletter

IN THIS ISSUE

Technical Articles

- Proximity Driven Exotic Phenomena at the Interface of Two Dissimilar Ground States
- Erection and Commissioning of Sodium Facility for Component Testing [SFCT]: A Multipurpose Sodium Loop

Young Officer's Forum

- Studies on Recycling the Solvent in Fast Reactor Fuel Reprocessing

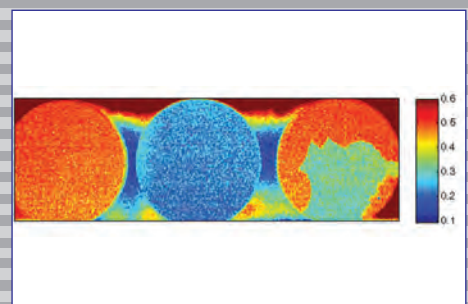
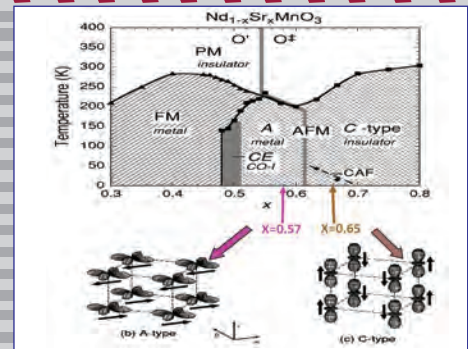
Young Researcher's Forum

- Evaluation of Coating Thickness and Debond in Thermal Barrier Coatings using Pulsed Thermography

Visit of Dignitaries

Forthcoming Meetings / Conferences

Awards & Honours



From the Editor

Dear Reader

This is the first issue of the newsletter in 2017. I take this opportunity to wish you all a very happy New Year.

It is my pleasant privilege to forward a copy of the latest issue of IGC Newsletter (Volume 111, January 2017 issue).

In the first technical article Dr. Awadhesh Mani and colleagues have discussed various aspects and results of proximity effect studies involving the interplay of superconducting ground states.

In the second technical article Shri P. Selvaraj and colleagues from Fast Reactor Technology Group have shared their experience on the erection and commissioning of a multipurpose sodium loop facility for component testing at Engineering Hall-I of Fast Reactor Technology Group.

This issue's young officer's forum features an article by Ms. Lavanya on studies on recycling the solvent in Fast Reactor Fuel Reprocessing.

Dr. Sharath has discussed on evaluation of coating thickness and debond in thermal barrier coatings using pulsed thermography in Young Researcher's Forum.

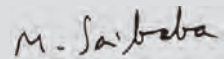
We had distinguished visitors to our Centre in the last quarter including, a delegation from United States Nuclear Regulatory Commission, led by Dr. Stephen Burns, Chairman, USNRC, Prof. A. K. Bhowmik, Professor of Eminence, RTC, IIT Kharagpur, Prof. Vijayamohanan K Pillai, Director, CECRI and Dr. Srikumar Banerjee, Homi Bhabha Chair Professor, DAE & Former Chairman, AEC

We are happy to share with you the awards, honours and distinctions earned by our colleagues.

We look forward to your comments, continued guidance and support.

With my best wishes and personal regards,

Yours sincerely,



(M. Sai Baba)

Chairman, Editorial Committee, IGC Newsletter

&

Director, Resources Management Group

New Year Message

Dear Colleagues,

I wish all colleagues of Indira Gandhi Centre for Atomic Research and their families, a very happy, prosperous, fruitful and professionally enjoyable New Year 2017.

It is extremely satisfying that, FBTR, in the 24th irradiation campaign, was operated at its highest power level of 26.1 MWt producing 5.2 MWe. Seventy two thorium subassemblies have been successfully loaded, after discharging steel subassemblies, in twelfth ring of the reactor core towards production of uranium-233. Neutron radiography of metallic fuel pin (Natural U-6Zr in T91 cladding) was carried out after test irradiation in FBTR to a burn-up of -3 GWd/t. Periodic safety review of KAMINI was completed and the reactor has now been licensed for operation till June 2020. KAMINI continues to provide excellent services in testing pyro-devices for all space launches of ISRO. Facilities for post-irradiation examination have been augmented for examination of advanced fuels and structural materials. Recent performance evaluation of MOX sphere-pac fuel pins and ferro-boron shielding material irradiated in FBTR have provided valuable insights into their irradiation behaviour. A new test reactor facility (FBTR-2) for continuing the material irradiation programmes beyond the life of present FBTR using metal fuel is being planned. Site for the proposed 100 MWt FBTR-2 has been identified and preliminary layout for the plant has been prepared in line with the experience from PFBR.

The commissioning of PFBR has made immense progress and we continue to extend our technical expertise and support. IGCAR and BHAVINI are working with great synergism towards obtaining the necessary regulatory and safety clearances. Some of the major contributions to PFBR include, updated reactor physics computations taking into account the actual fuel fabrication parameters, estimation of site boundary dose, probabilistic safety assessment studies for internal and external events, comparative reliability analysis of Safety Grade Decay Heat Removal System (SGDHR) with and without electro-magnetic pump, seismic qualification of important reactor systems such as sodium-air heat exchanger (AHX) in the SGDHR system, structural analysis of sodium piping systems in the as-built condition, checking and ensuring the adequacy of line heaters on the sodium piping, commissioning and performance checking of various component handling systems, systematic commissioning of various airlocks, etc. The effect of sodium aerosols on the performance of in-vessel fuel transfer machine of PFBR was ascertained by testing it under simulated reactor operating condition. We have also evolved a new methodology based on glancing angle ultrasonic imaging for mapping the sub-assembly heads in PFBR. It was indeed a major achievement to be able to complete the required pre-service



tube inspection of all the eight PFBR Steam Generators using the state-of-the-art in-house developed robotic device, the PFBR Steam Generator Inspection System (PSGIS). Also, the robotic inspection device for the roof slab to main vessel dissimilar metal weld DISHA has now been upgraded for carrying out pre-service inspection at the required elevated temperature. Both these pre-service inspection devices should now satisfy the necessary regulatory requirements for commissioning of PFBR.

We have made significant progress in the design of 600 MWe future FBRs which will be deployed as twin unit reactors. Conceptual design of major systems for FBRs 1&2 was completed incorporating the latest design standards with a view to totally eliminate accidents. In parallel, state-of-the-art design safety criteria for MOX fuelled future FBRs are being finalized in collaboration with AERB, invoking post-Fukushima and Gen-IV safety standards. A processor based CPU card has been indigenously designed and developed for diversified real time computer systems for future FBRs in collaboration with ANURAG, DRDO. A unique experimental facility has been developed in-house, to assess the effect of stress fluctuations on creep behavior of reactor structural materials.

CORAL continued to operate and reprocess the spent fuel of FBTR. One of the significant achievements has been the in-situ replacement of degraded radiation shielding window, which has been carried out for the first time with minimum man-REM expenditure. The construction activities are nearing completion at DFRP. Successful demonstration of pyrochemical reprocessing of U-Zr fuel (100 gram) in a hot cell facility has been a significant milestone.

Construction of the Fast Reactor Fuel Cycle Facility (FRFCF) and fabrication of major components have gained momentum during the year. FRFCF would continue to be a project of priority to the Centre and all the efforts would be made to ensure the speedy progress of this project.

A significant number of experimental facilities have also been commissioned during the current year, notably the large scale (5/8th) water-model test facility at Engineering Hall-IV for hydraulic studies and validation of design concepts for the future FBRs, facility based on travelling heater method for growing single crystals of CdZnTe (CZT) for application in room temperature semi-conductor radiation detectors and advanced dual beam ion irradiation facility comprising indigenously built 400 kV accelerator (for injecting helium), 1.7 MV Tandem accelerator (for irradiation by heavy ion beam), etc. A new experimental sodium loop (Sodium Facility for Component Testing) for testing small and medium sized components with state-of-the-art features is in an advanced stage of commissioning. An indigenous fully automated Waste Assay Computed Tomography (WACT) nested modeling system, atmospheric dispersion studies and a decision support system for nuclear emergencies for national, regional and local scale has been developed. Multi-purpose high-performance parallel computing cluster with 180 teraflops has also been commissioned. RFID cum biometric based physical access control system has been designed and deployed in radiological facilities. We have developed a lung tissue equivalent polymeric material and a silicone rubber mould for Lawrence Livermore National Laboratory (LLNL) lung and succeeded in innovating methodology for gross leak detection in fabricated components using infrared thermography, characterization of grain size variation in austenitic stainless steel using non-linear ultrasonics and application of Total Quality Management based approach in Non Destructive Examination during construction of nuclear piping facility.

A significant milestone was achieved when the BARC Training School at IGCAR successfully completed its tenth year and young qualified scientists and engineers were placed in various Units of DAE. In the current batch, 36 Trainee Scientific Officers are undergoing training. As a constituent institution under Homi Bhabha National Institute, our Centre at present has 153 research

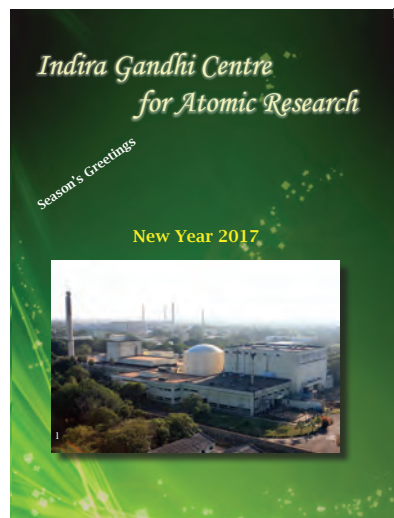
scholars pursuing their doctoral programmes. Further, 215 students belonging to different institutes from all over the country have pursued their post-graduate project work at our Centre. This year, a total of around 1300 visitors, comprising students, faculty and public have visited our Centre. Many foreign and national dignitaries have also visited our laboratories and the campus.

The year ahead would require committed efforts by all the colleagues towards achieving the various targets with respect to the Second Stage of India's nuclear energy programme and the associated fuel cycles as envisaged in the Vision Documents submitted to NITI Aayog by the Department. Notable among them are the finalization (in collaboration with BHAVINI) of the Preliminary Design Report for the 600 MWe FBRs 1&2 as also of the Conceptual Design Report for FBTR-2. It is now decided that the FBTR-2 will be metallic fuel driven and both aqueous (on the short term) and pyro (on the long term) reprocessing of the metallic fuel would be pursued as a precursor to the deployment of metallic fuel driven FBRs. Therefore, it is essential that the necessary Metallic Fuel Fabrication Facility (MFFF) and metallic fuel reprocessing activities will have to be pursued with a sense of urgency. This will necessitate inter-disciplinary efforts involving all the Groups at the Centre so that IGCAR remains in the forefront internationally in the domain of closed fuel cycle fast reactor technology. It shall also be our endeavour to groom and mature young scientific, engineering and technical colleagues of the Centre to enable them to take up higher responsibilities in the medium term.

Looking forward to working synergistically along with our colleagues in Administration, Accounts and CISF, in a cooperative and friendly atmosphere, for a productive and professionally rewarding year ahead to ensure sustained growth of our Centre.

Arun Kumar Bhaduri
30/12/2016

(Arun Kumar Bhaduri)
Director, IGCAR



Proximity Driven Exotic Phenomena at the Interface of Two Dissimilar Ground States

The subtle condensation of tiny atoms, consisting of merely electrons and nucleons, has been at the helm of the genesis of condensed media which have culminated in myriad forms of the interesting systems adorned with distinguished physical properties. The state of a system with unique characteristic property acquired at absolute zero temperature is referred to as its ground state. Starting from a simple system such as normal metal, conventional insulator to complicated ones like heavy fermions, Kondo insulators, superconductors, magnetic and ferro-electric systems are examples of a few among the many interesting ground states prevailing in the condensed medium. Subsequent discoveries of complex systems comprising more than one ground state, e.g., magnetic superconductors, multi-ferroics and manganites etc., have brought new dimension in the research arena of condensed matter physics. This has provided a clue to researcher to explore the possibility of artificial design of heterostructures by bringing two dissimilar ground states, which do not coexist otherwise, in an intimate contact and study the evolution of modified physical properties of composite ground states across the interface. This novel idea has opened a new field of research topic popularly referred to as proximity effect, which over the period of time has proven not only interesting on basic research point of view but also possesses immense potential to be harnessed for technological applications.

Figure 1 provides a schematic view of a heterostructure formed at the interface where two systems, namely A and B, each representing a distinct ground state, have been placed in a close contact. Under proximity effect, the electronic wave function of system A(B) permeates into the territory of the system B(A) through the interface up to a certain characteristic length ξ_B (ξ_A). This process of mutual transgression of the territories of respective systems by their rival electronic wave functions leads to a substantial modification of the physical properties of both the systems in the vicinity of the interface extending from ξ_B to ξ_A (Figure 1). The magnitude of ξ_B (ξ_A) is dictated by the interaction strength and the nature of the two systems in contact as well as the quality of the interface. Among the two systems involved in the proximity effect related studies, a superconductor is quite often selected as one of the systems while the other system can be a normal metal, magnetic or topological system. The ground state of a conventional superconductor emerges on account of subtle pairing of electrons of opposite spins as well as equal and opposite orbital momentum (called Cooper pairs) where participant quasi-electrons lose their Fermionic character in favour of formation of macroscopic Bosonic condensate. In superconducting state, a material completely loses its electrical resistivity and acquires perfect diamagnetism. The pair wave function of a superconductor

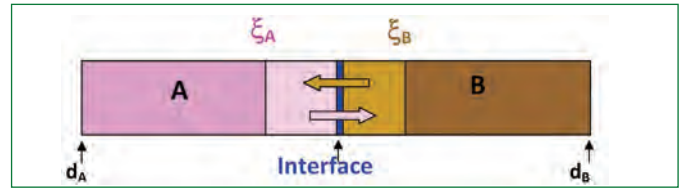


Figure 1: Schematic view of a heterostructure formed by systems A and B. ξ_A and ξ_B are characteristic lengths and d_A & d_B are thicknesses of A and B respectively

with its well defined coherence length (ξ) has the ability to penetrate into the other material in its closed proximity, and hence, becomes one of the most suitable candidates for such studies. Before we proceed to bring out some of our studies performed on heterostructures comprising a high temperature superconductor and various types of magnetic phases of manganites, it is useful to give a brief account of the general outcomes of proximity studies involving rather simpler systems, such as a superconductor–normal metal and superconductor–magnetic systems, which may provide necessary background for an understanding of the present subject.

Proximity Effect in Superconductor–Normal Metal (SC/NM) System

The SC/NM interface provides a simple system to study the interplay of superconductivity and a normal metal in contact. The Cooper pairs emanating from superconductor side penetrate the normal metal over a certain distance ξ_N . The magnitude of ξ_N is different in two different limiting cases: First, if the electron's motion is diffusive, (i.e., in dirty limit), ξ_N is proportional to the thermal diffusion length scale $L_T \sim \sqrt{(D/T)}$ where D is the diffusion constant. Second, for a pure normal metal (i.e. in clean limit) the corresponding characteristic distance is $\xi_N \sim v_F/T$, where v_F is Fermi velocity of electron. In either of the cases, the Cooper pairs entered in normal metal tend to induce superconducting like properties in the normal metal. This phenomenon is called the proximity effect. Simultaneously the leakage of the Cooper pairs weakens the superconductivity of the superconductor layer over a coherence length of ξ_S near the interface. This effect is called the inverse proximity effect. The latter effect results in a decrease of the superconducting transition temperature (T_C) in a thin superconductor layer in contact with the normal metal. If the thickness of a superconductor layer is smaller than a critical one, the proximity effect totally suppresses the superconducting transition. In a nutshell, in SC/NM structure, superconductor changes the property of normal metal by inducing superconductivity in the latter. Concomitantly, the normal metal also affects the property of a superconductor by suppressing its T_C in the vicinity of the interface.

Proximity Effect in Superconductor–Ferromagnet (SC/FM) System

The singlet superconductivity and ferromagnetism are two antagonistic long range orders. Therefore, their coexistence in bulk compound is highly unlikely. However, they can be brought together in artificially designed bilayers of Superconductor–Ferromagnet (SC/FM) structure. We know that in ferromagnets electrons with spins up and spin down belong to two different energy bands. The energy shift between the spin-up and spin down bands gives rise to an effective exchange field (h), which acts on the spin of any foreign electron which enters in ferromagnet regime. In most superconductors the wave function of the Cooper pairs is singlet, i.e., the electrons of a pair have opposite spins. As Cooper pairs penetrate into ferromagnet regime, its exchange field tries to align the spins of the electrons of a Cooper pair parallel to each other. This leads to breaking of Cooper pairs and hence, causes the superconducting order parameter to decay in the ferromagnet layer within a length scale ξ_F as a consequence of direct proximity effect. Simultaneously, the leakage of the Cooper pairs weakens the superconductivity in superconductor layer within a characteristic length scale ξ_S , which is of the order of the superconducting coherence length. The superconducting condensate decays faster in the ferromagnet region than that in NM region. Based on the strong suppression of the superconductivity in the SC/FM systems, one should not construe that the proximity effect in SC/FM structures is less interesting than that in SC/NM systems. In fact, a great deal of exotic phenomena has been observed on account of interplay of SC & FM. It is observed that the Cooper pair wave function extending from SC to Ferromagnet, does not simply decrease exponentially, but exhibit damped oscillatory behavior as a function of ferromagnet layer's thickness. Consequent to this, there emerges a great deal of new phenomena, such as spatial oscillations of the electron density of states (DOS), non-monotonic variation of the T_C of SC/FM bilayers as a function of ferromagnet layer thickness, and the realization of “ π ” Josephson junctions in SC/FM/SC systems. All these phenomena cannot be perceived based on the common wisdom of simple prevalent theory. Spin-valve behavior in complex SC/FM structures gives another example of the interesting interplay between magnetism and superconductivity, an effect that is promising for potential applications.

Proximity Effect in a High Temperature Superconductor (HTSC) and a System with Multiple Magnetic Ground States

So far we have presented the important findings of interaction between two systems, each with a single ground state (GS), i.e., a conventional superconductor with a NM or a FM. The interplay of magnetism and superconductivity becomes far more complex when it involves a system with multiple magnetic GS such as the half metallic manganites coupled with

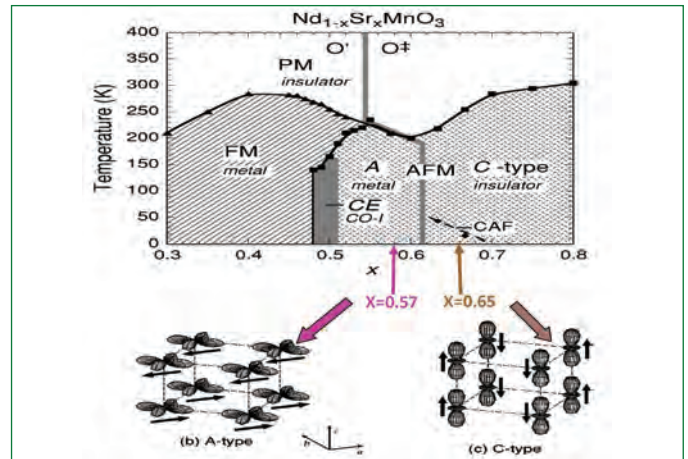


Figure 2: (a) Phase diagram of $Nd_{1-x}Sr_xMnO_3$. The details of spin arrangements on a unit cell are shown for (b) A-type AFM ($x=0.57$) and (c) C-Type AFM ($x=0.65$)

nonconventional high temperature superconductors (HTSC). A colossal magnetoresistance (CMR) material belongs to a category of half metallic manganite system which possesses a variety of rich magnetic ground states. Therefore, its combination with a HTSC forms an interesting but challenging research problem. Fortunately, the CMR materials have excellent chemical & structural compatibility with high- T_C superconductors to form good heterostructures. The short coherence length of HTSC is suitable for retaining superconductivity in very thin layer and hence, facilitating the investigation of interplay between ferromagnet and superconductor very close to the interface. In addition, high degree of spin polarization of CMR materials in conjunction with d-wave pairing symmetry of HTSC provide good avenues of investigating spin dependent effects in transport, probing of unconventional superconductivity and for modifying superconducting properties. Apart from basic research, these heterostructures are also envisaged to be prospective candidates for technological applications in designing of new superconducting devices such as spintronic devices. In these devices, instead of charge of electrons their spins are exploited for operational purposes. Spin devices, consisting of superconducting layer sandwiched between two ferromagnetic layers, require an antiferromagnetic (AFM) inter layer to pin the spins of one of the ferromagnetic layers. Therefore, the detailed understanding of proximity effect in AFM/SC as well as FM/SC system is useful towards the realization of such devices.

In what follows, we present a brief account of the proximity effect related studies performed by us on heterostructures consisting of a HTSC, namely, $YBa_2Cu_3O_7$ and a manganite, $Nd_{1-x}Sr_xMnO_3$. It is evident from the phase diagram shown in Figure 2a that $Nd_{1-x}Sr_xMnO_3$ (NSMO) exhibits a variety of magnetic ground states. It has FM metallic GS for $x < 0.48$; charge ordered CE-type AFM for $0.48 \leq x \leq 0.52$; A-type AFM for $0.48 \leq x \leq 0.62$; C-type AFM insulating GS for $x > 0.62$ and coexistence of Canted AFM with C-type AFM for $0.62 \leq x \leq 0.7$. We have chosen two specific

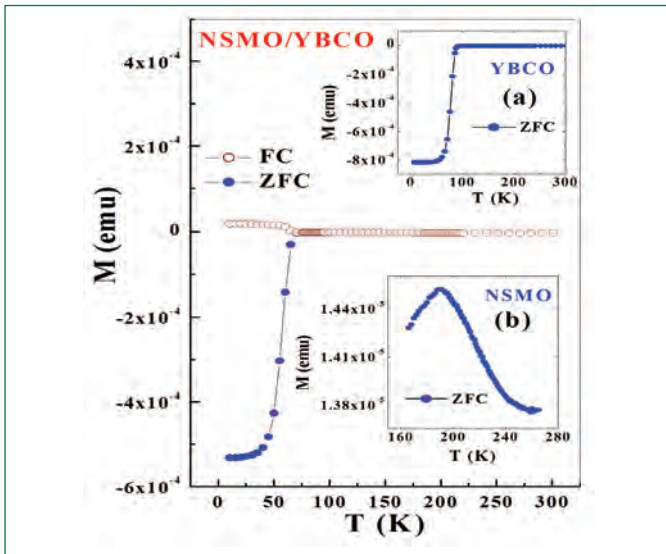


Figure 3: Magnetization (M) vs temperature (T) curve for NSMO_A/YBCO bilayer. The M-T curves for YBCO and NSMO are shown in the upper and the lower insets, respectively, for ZFC data

compositions of NSMO namely $x=0.57$ & 0.65 and fabricated bilayer thin film structures of YBa₂Cu₃O₇/ Nd_{0.43}Sr_{0.57}MnO₃ and YBa₂Cu₃O₇/ Nd_{0.35}Sr_{0.65}MnO₃, preferentially grown along c-axis over LaAlO₃ (LAO) substrates using pulsed laser deposition system, to investigate proximity effect in these systems. A succinct description of the two systems is given below.

(a) Proximity Effect Studies in the Nd_{0.43}Sr_{0.57}MnO₃/YBa₂Cu₃O₇ Heterostructure

The magnetic GS of the chosen composition of Nd_{0.43}Sr_{0.57}MnO₃ (designated as NSMO_A) is a A-type antiferromagnet (AFM). In the A-type AFM the electron spins are ordered ferromagnetically in the ab-planes with the magnetic moments pointing toward a-axis and the ab-planes are stacked antiferromagnetically along the c-axis (Figure 2b). It is thus expected that the carriers confined in the ab-planes of NSMO_A may be spin polarized and may generate interface spin-injection effect. Therefore, NSMO_A in conjunction with YBa₂Cu₃O₇ (YBCO) provides an ideal system facilitating twin objectives of studies: (i) to investigate the effect of A-type AFM on d-wave pairing superconductors & vice versa and (ii) exploring the possibility of polarized spin injection from ab-planes of NSMO into YBCO & its effect on SC properties of the latter.

Salient features of the main finding of the above studies :

Temperature dependent magnetization (M-T) measurements have been performed on NSMO_A/YBCO as well as NSMO_A & YBCO single layers. M-T curves (Figure 3) reveal that the T_c for the YBCO single layer is 88 K and Neel Temperature (T_N) for the NSMO_A single layer is 195 K. For the NSMO_A/YBCO bilayer while T_N remains at 195 K, the T_c of bilayer decreases to 82 K. The suppression of T_c of bilayer under the proximity effect of A-type AFM of NSMO_A is interpreted to arise due to the nesting features of Fermi surfaces of AFM band which causes the symmetry-breaking in momentum

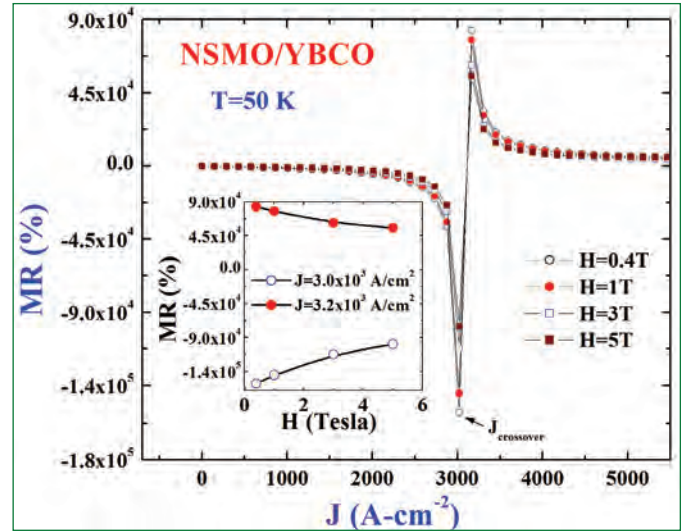


Figure 4: Variation of MR as a function of current density (J) at a fixed temperature of 50 K at various magnetic fields ranging from H=0.4 to 5 T. Inset shows MR vs H for $J=3.0 \times 10^3$ and 3.2×10^3 A cm⁻² exhibiting crossover from negative to positive MR

space, similar to the splitting of the Fermi surface in the FM case. The magnetoresistance (MR), [defined as $MR = [\rho(H) - \rho(0)] / \rho(0)$, where $\rho(H)$ & $\rho(0)$ are resistivity at the magnetic field of 0 & H Tesla respectively], performed up to the magnetic field H= 5T on NSMO_A/YBCO and the corresponding single layers also reveal quite interesting results. The MR of NSMO_A/YBCO is observed to be positive for temperature below T_c while the MR of pure NSMO_A is negative at the same temperature. This demonstrates a reverse proximity effect in which superconductivity plays a dominant role in dictating the MR behavior of the heterostructure.

Another outstanding finding of this study is the current density (J) biased injection of polarized spin carriers from NSMO_A layer into YBCO leading to strong suppression of T_c across the interface. MR measurements at various biased current densities, J ranging from 3.75×10^2 to 4.5×10^4 A/cm² (Figure 4) reveal that the suppression rate of T_c with respect to J, [i.e. (dT_c/dJ)] in NSMO_A/YBCO is about three orders of magnitude larger than that in the YBCO single layer. This suggests that the current-induced pair-breaking effect is more severe in NSMO_A/YBCO than in the pure YBCO, as J biasing is increased. Such a huge suppression of T_c cannot be realized solely based on exchange field of A-type AFM of NSMO_A. This can be rationalized based on the fact that the increase in J leads to an increase in the injection of spin polarized carriers from ferromagnetic ab-planes of NSMO_A into YBCO across the interface of NSMO_A/YBCO. It is known that polarized spin injected in a superconductor has strong Cooper pair breaking effect and hence, causes severe suppression of T_c. The present study for the first time has demonstrated and brought about a new idea of J biased spin injection system which may be used in future for realization of spin injection devices.

An offshoot of the present study is a spectacular switching

of the MR from a huge negative value of $\sim 10^5$ to a colossal positive value of 8×10^4 % around a crossover current density of $J_{\text{crossover}} \sim 3.02 \times 10^3 \text{ A cm}^{-2}$ (Figure 4). The inset of Figure 4 shows the variation of MR as a function of H at various J close to the crossover region. For $J \leq J_{\text{crossover}}$, MR is negative and increases with increasing H. In contrast, for $J \geq J_{\text{crossover}}$, MR is positive and decreases with increasing H. This indicates that current density profoundly affected the evolution of MR in the present bilayer system. To our knowledge, such a large MR and its dependence on current density as observed in our sample has not been reported in any other bilayer systems.

(b) Proximity Effect in the $\text{Nd}_{0.35}\text{Sr}_{0.65}\text{MnO}_3/\text{YBa}_2\text{Cu}_3\text{O}_7$ Heterostructure

The chosen composition of NSMO_C exhibits two distinct magnetic ground states: (i) C-type AFM below Neel temperature, $\sim 250 \text{ K}$ in which electron spins aligned ferromagnetically along c-direction are antiferromagnetically coupled in a-b plane. (ii) By further lowering the temperature, a FM order appears due to the canting of spins below a transition temperature, $T_{\text{CAF}} \sim 35 \text{ K}$ (Figure 2). Hence, the present combination of $\text{Nd}_{0.35}\text{Sr}_{0.65}\text{MnO}_3/\text{YBa}_2\text{Cu}_3\text{O}_7$ [designated as $(\text{NSMO}_C/\text{YBCO})$] heterostructure provides a good avenue for exploring the coexistence and interaction of superconductivity with a CMR system comprising two long range magnetic ground states, namely C-type AFM followed by FM orders emanating from the same source (NSMO_C).

Figures 5a and 5b display the $\rho(T)$ of $\text{NSMO}_C/\text{YBCO}$ at various H and NSMO_C at zero field respectively. The positions of Neel temperatures in NSMO_C single layer and $\text{NSMO}_C/\text{YBCO}$ bilayer are marked by arrows in Figure 5b and the upper inset of Figure 5a respectively. NSMO behaves as an insulator and its $\rho(T)$ exhibits a dip near T_{CAF} . It is interesting to see that $\text{NSMO}_C/\text{YBCO}$ exhibits double transition corresponding to two distinct magnetic ground states of NSMO_C . First it shows superconducting transition with zero-resistance around $T_c = 60 \text{ K}$. Clearly the T_c of bilayer is much lower than the value of single layer YBCO ($T_c = 88 \text{ K}$) due to the proximity of C-type AFM of NSMO_C . Second transition occurs at $T_{\text{CAF}} \sim 35 \text{ K}$ when NSMO_C acquires ferromagnetism due to canting of spins. This leads to complete suppression of superconductivity of the bilayer leading to re-emergence of finite resistivity at T_{CAF} . The field dependency of $\rho(T)$ in $\text{NSMO}_C/\text{YBCO}$ shows a typical shift toward low temperatures, which is attributed to the vortex-dissipation due to the internal magnetic field from the magnetic moments of the spin-canting state. Another transition appears at $T_{\text{re}} \sim 24 \text{ K}$ where Superconductor re-appears with zero resistivity. This is called re-entrant superconductivity, which in the present scenario arises due to overcoming of Superconductor order parameter over the ferromagnetic spin-canting state of NSMO_C as the temperature is lowered. Such multiple transitions clearly indicate intense competition between the two long range ordered ground states across the interface.

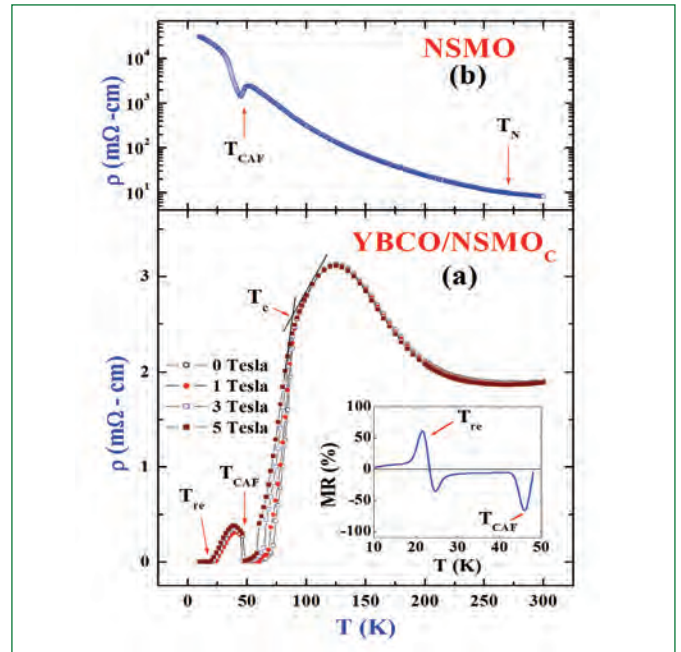


Figure 5: (a) and (b) plot the temperature dependent resistivity $\rho(T)$ $\text{YBCO}/\text{NSMO}_C$ bilayer & NSMO_C , respectively. The inset in (a) displays the temperature dependent MR measured at a moderate field of 1T

The distinct changes of $M(T)$ and $\rho(T)$ near T_{CAF} and T_{re} are also reflected in their magnetoresistance behavior as shown in the inset of Figure 5a, with MR-value defined as $[\rho(1\text{Tesla}) - \rho(0)]/\rho(0)$. The MR-value is negative with a maximum of -46% near T_{CAF} and it switches over to a positive value of $\sim 60\%$ around T_{re} . The negative MR in the normal state region is consistent with the picture that the magnetic field enhances the spin ordering and hence, reduces the spin scattering contribution to the resistivity. As to the positive MR-value in the superconducting regime, it could be due to a combination of many factors including

- (1) The Aslamazov-Larkin (AL) term arising from the fluctuation of Cooper pairs
- (2) The regular and anomalous Maki-Thompson (MT) contribution originating from the coherent scattering of a Cooper pair
- (3) The correction of density of states (DOS) in association with the formation of bound fluctuated pairs
- (4) The vortex dissipation.

In summary, a brief description of various facets & outcomes of proximity effect studies involving the interplay of a superconducting (conventional as well as non-conventional) ground states with a few selected systems such as NM, FM and CMR comprising single as well as multiple long range magnetic ordered ground states have been presented. The objective of this presentation was to give a general feel about the excitement, intricacies & richness of the ongoing research activities in areas of proximity effects across the interface of two competing long range ground states.

*Reported by
Awadhesh Mani and Colleagues
Materials Science Group*

Erection and Commissioning of Sodium Facility for Component Testing [SFCT]: A Multipurpose Sodium Loop

A new dynamic state of art sodium loop with three test vessels, heater vessel, heat exchangers and purification circuit has been erected in our Centre. This loop, named as "Sodium Facility for Component Testing (SFCT)" is a multipurpose sodium loop and will be used for sodium testing of scaled down components of future FBRs. Experimental studies which are part of developmental activities in sodium technology for FBRs, are also planned to be conducted in SFCT. The material of construction of the components and piping in this facility is SS 316LN grade austenitic steel. The maximum operating temperature of SFCT is 550°C

The objectives of the facility is testing and calibration of medium length (≈ 5000 mm) MI type continuous/discrete sodium level probes and RADAR level probes, in-sodium testing of small and medium size components which are subsystems of reactor, testing of different types and capacities of EM Pumps developed in FRTG, testing and calibration of permanent magnet and ultrasonic flowmeters, sodium freezing studies simulating the secondary circuit of FBRs, testing of sweep arm ultrasonic under sodium scanner and testing of sensors being developed in IGCAR as part of In Service Under Sodium Examination (INUSE).

Features of sodium facility for component testing are three test vessels of different sodium capacities, 50 m³/h capacity EM pump maintaining sodium flow in the heating and cooling circuit, 170 m³/h capacity EM pump for experiments at low temperatures (<450°C) with large flow requirement, heating and cooling circuit with sodium to air heat exchanger, heater vessel and economiser heat exchanger, cold trap for sodium purification, plugging indicator for impurity monitoring, sodium storage / dump tank in dump pit



Figure 1: (a) Argon Header of sodium facility for component testing and (b) Compressed air system header of SFCT

[2 metres depth] with 1.4 metres dyke above FFL (9.3 metres) and related cover gas and compressed air circuits.

Special features of sodium facility for component testing are test section for corrosion and erosion studies, pump test section, test section for sodium freezing studies and test section for permanent magnet and ultrasonic flow meters calibration.

PRE-Commissioning Activities

As part of commissioning of SFCT, various systems were checked for their performance before integrating the individual systems. Following are the details with respect to individual systems.

Argon Cover Gas System

The argon cover gas system comprising argon gas manifold, purifier unit and cover gas header was checked for its operating performance. The pressure regulators, gauges, transmitters and pressure relief valve in the system were checked. The diaphragm valves and vacuum pumps in the system were also checked for smooth operation. The operations such as venting, evacuation and pressurizing of storage tank, loop and test vessels were carried out



Figure 2: Piping of sodium facility for component testing

through cover gas system. The oxygen and moisture content in argon gas coming out of argon purifier unit were checked using oxygen and moisture meters. The measured values of oxygen and moisture were 10 and 12 ppm respectively. Figure 1a gives the photograph of argon header.

Compressed Air System

The compressed air system comprising air compressors, air dryer and air header was checked for its operating performance. The pressure regulator, gauge, transmitter and pressure relief valve in the system were checked. Smooth operation of air compressors and cut-in/cut-off pressures were checked. Functioning of automatic condensate drain valve in the compressor was also checked. The diaphragm valves in the system were checked for smooth operation. The dew point of compressed air coming out of air dryer was checked using dew point meter. The measured value of dew point of dry air was -42.5°C (95 ppm). Figure 1b gives the photograph of compressed air system header.

Pressure Hold Test of Sodium Loop

Pressure hold test of loop, test vessels and storage tank was conducted at room temperature for a period of 24 hours using argon gas at 1 kg/cm^2 (g). No pressure drop was noticed in storage tank, loop, Test Vessel-1 [TV-1] and Test Vessel-2 [TV-2]. However, in Test Vessel-3 [TV-3] the pressure drop observed was 0.024 Kg/cm^2 (g) which is within acceptable limit.

Cold Purging of Sodium Facility for Component Testing

Cold purging of loop, test vessels and storage tank was carried out at room temperature using argon gas. Four cyclic purging operations with pressure range of -0.9 and 1 kg/cm^2 (g) were carried out. The oxygen and moisture content in argon gas in loop, test vessels and storage tank were measured using oxygen and moisture meters. The measured values of oxygen content in argon gas in loop, TV-1, TV-2, TV-3 and Storage Tank were 15, 103, 10, 20 and 100 ppm respectively.

The measured values of moisture content in argon gas in loop, TV-1, TV-2, TV-3 and Storage tank were 27, 19, 18, 24 and 30 ppm respectively.

Load Hangers Checking

Variable spring hangers, tie rods and rigid supports provided in the pipe lines were checked for proper location based on flexibility analysis. The cold load of variable spring support hangers was set as required.

Valves Checking

All bellows sealed sodium valves viz., pneumatic, motorized and manual type were checked for smooth operation and functioning of position indication in control room was also cross checked.

Electrical & Instrumentation Systems

Power control centers, Motor control centers, Heater control panels, Emergency control panel, control room electrical panels, EM pumps, air blowers and Class-I, Class-II and Class-III power supply systems were commissioned. The healthiness of all surface and immersion heaters was checked. The emergency lighting system was also commissioned. Control room instrumentation panels, Field instrumentation panels, Remote input/output panels and DACS panel were commissioned. Cover gas and compressed air pressure measurement system, sodium flow and sodium temperature measurement systems, sodium level detection system, sodium leak detection system and data acquisition and control system were also commissioned. Various control logics provided for the safe operation of the system was checked for its proper functioning.

Hot Purging of SFCT

Preheating of loop was initiated after switching on the electrical panels. To start with, storage tank components and piping in the loop and heaters were switched on and once temperature reached 200°C , hot purging of the tank was completed. Subsequently, after achieving the required temperatures in the test vessels, loop and components, hot purging operation was carried out and completed. Consequent to hot purging, the oxygen and moisture content in the loop reached 10 and 30 ppm respectively which is well within the acceptable limits. Figure 2 gives the photograph of the piping in the loop. Figure 3 gives the flowsheet of the loop.

Preheating of Transport Tank

Transport tank containing around 5.5 tonne of sodium was shifted from Engineering Hall-III. Preheating of this tank has been initiated and the temperature of sodium in the tank has reached 160°C .

Commissioning Work in Progress

Six tonnes of sodium from the transport tank has been transferred in to the Storage Tank and it is planned to fill sodium in the loop shortly, check for impurities, purified and brought in to operation.

SFCT, a multipurpose sodium loop has been erected and commissioned at Engineering Hall-I of FRTG. Testing of components will be initiated shortly. This test facility will provide impetus to mandate on testing of components for future Fast Breeder Reactors.

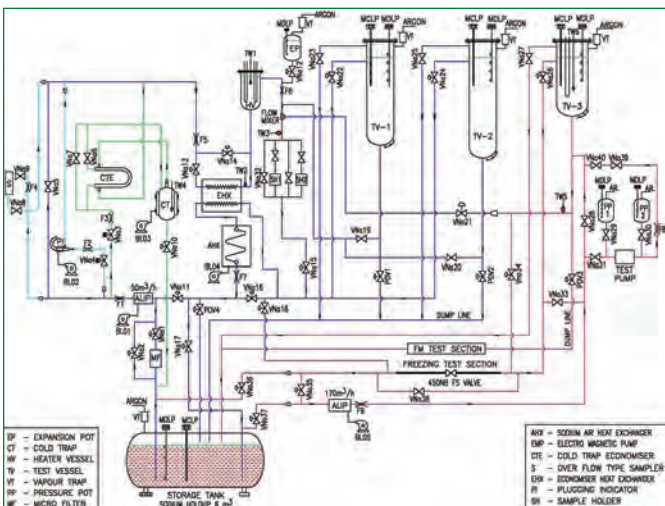


Figure 3: Flow sheet of sodium facility for component testing

Reported by

P. Selvaraj and Colleagues

Fast Reactor Technology Group

Young Officer's FORUM

Studies on Recycling the Solvent in Fast Reactor Fuel Reprocessing

Thirty percentage tri-n-butyl phosphate/n-dodecane is used as the solvent in the aqueous reprocessing of spent fuel from a nuclear reactor. Fast Reactor Fuel Reprocessing (FRFR) involves handling of much higher concentrations of Pu, as compared to Thermal Reactor Fuel Reprocessing (TRFR). The specific activity handled is also much higher in the case of FRFR (of the order of 1000 Ci/L) as compared to TRFR (of the order of 200 Ci/L). Thus, the solvent used in fast reactor fuel reprocessing undergoes higher degradation due to increased radioactivity. The degraded products not only retain plutonium, but also retain other fission products. As a result, the overall decontamination factor reduces and the phase separation time increases. This hampers the reuse of solvent.

The solvent degradation and solvent treatment in thermal reactor fuel reprocessing is known for several years. In thermal reprocessing plants the solvent is reused after treating with sodium carbonate. The treated solvent is being used for six times, thereby reducing the organic waste to the maximum. However, unlike thermal reprocessing, though the process followed and the solvent used are same, this process for treating the solvent is just not sufficient in fast reactor fuel reprocessing because of its higher degradation. This calls for an alternate method of treatment.

The objective of this work is to develop a process to treat the solvent used in FRFR and qualify it for reuse. This would minimize the waste stream volume, decrease the accumulation and storage

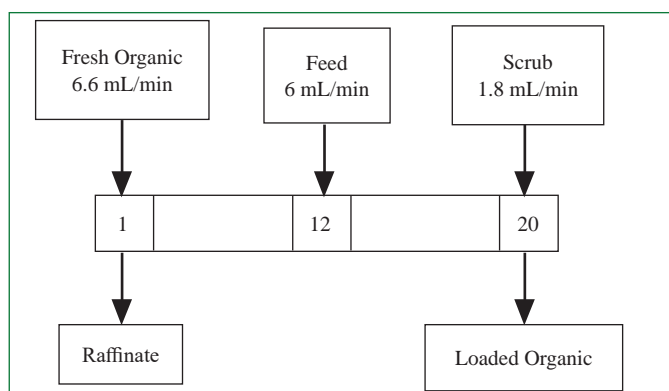


Figure 1: Flowsheet for extraction studies



Ms. A. L. Lavanya is working in the Plant Operation Section of Reprocessing Group. She is from the 8th batch of BARC Training School at IGCAR Campus and joined the Group in 2014. She did her B.Tech in Chemical Engineering from Osmania University and completed M.Tech. in Nuclear Chemical Engineering from HBNI in 2015.

constraints and makes the process more economical.

The lean solvent from the PUREX process will contain unstripped plutonium, uranium and degraded products of tri-n-butyl phosphate and dodecane. The solvent needs to be treated to recover the valuable heavy metals and remove the degraded products. The treated solvent is tested for the phase separation time, plutonium retention, concentration of di-n-butyl phosphate and interfacial tension. If these values are nearly equal to those of a fresh solvent, the treated solvent is used for extraction studies with a simulated feed solution containing plutonium and uranium followed by stripping operation of the loaded solvent (Figure 1).

Experimental Setup

The treated solvent was used for extraction and stripping studies in a 20 stage air pulsed ejector mixer-settler. Figure 2 displays the flowsheet for the stripping studies. The feed was given at the 12th stage. The solvent was fed from the 1st stage and scrub was sent from the 20th stage. Stages 1 to 12 formed the extracting section and stages 13 to 20 formed the scrubbing section. The flow ratio of feed: solvent: scrub was set as 1 : 1.1 : 0.3.

The loaded organic was fed in the 1st stage. Strip 1 was 4 normal nitric acid, which was given at the 10th stage. Strip 2 was 0.01 normal nitric acid which was given at 20th stage. The flow ratio of loaded organic: strip1: strip2 was maintained as 1 : 0.15 : 1.4.

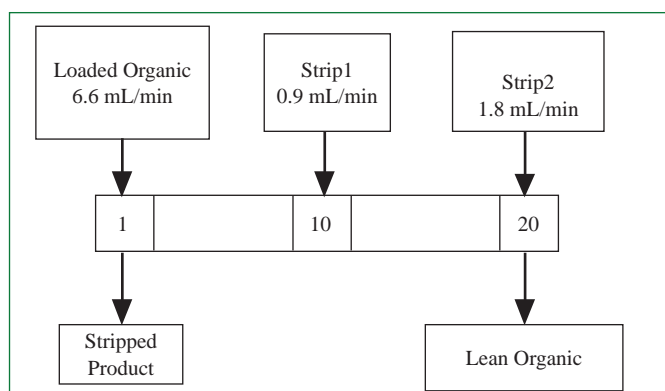


Figure 2: Flowsheet for stripping studies

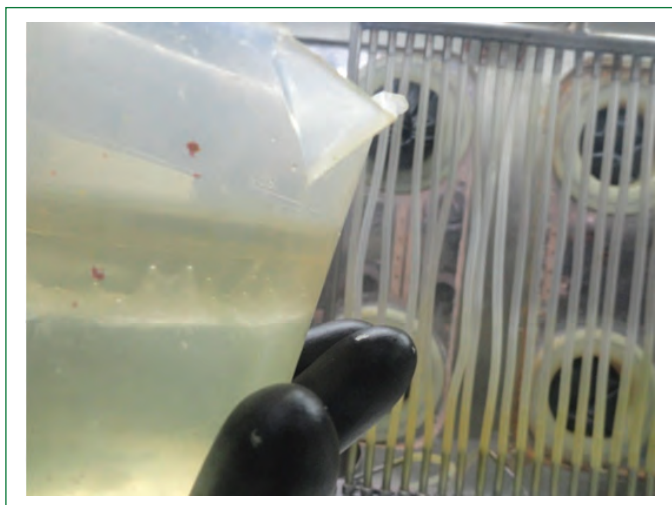


Figure 3: Crud formation during stripping operation

Recovery of Plutonium

For recovering plutonium the lean solvent was treated with 0.2M oxalic acid in a single stage mixer settler with aqueous and organic flow ratio of 1:1. Oxalic acid removed nearly all the plutonium from the lean organic solvent in one contact.

Hydrazine Carbonate Treatment

After recovering plutonium, the solvent was treated with 15% hydrazine carbonate degraded products of tri-n-butyl phosphate could be largely removed. Depending upon the concentration of di-n-butyl phosphate, the number of contacts required can be decided. For concentrations of di-butyl phosphate less than 500 ppm, single contact was sufficient for its removal.

The solvent was qualified on the basis of phase separation time, plutonium retention, concentration of di-butyl phosphate and interfacial tension. The solvent after treatment extracted plutonium and uranium well enough from the feed solution as equal as the fresh solvent, but during stripping operation, a crud was formed possibly due to diluent degraded products which posed operational difficulty (Figure 3).



Figure 5: Crud formed during Mixer-Settler runs

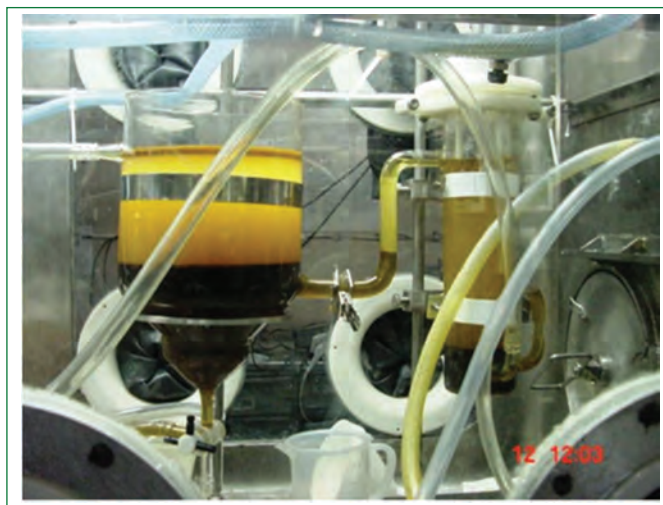


Figure 4: Solvent treatment setup

Treatment using Resin

An adsorbing process was tested utilizing the Dowex Resin. The resin was loaded into a column with demineralised water. 5% NaOH solution was passed through the column so as to replace all the chloride ions with hydroxide ions. The colour of the resin changed from white to brown. After this, the resin was washed with demineralised water to remove all the free hydroxide ions. The resin was left open to air dry and the dried resin was loaded into a column with dodecane. The solvent treated was passed through this column at a very low flow rate. Significant change in phase separation time was observed after this treatment. The treated solvent after passing through a resin showed significantly less amount of crud during stripping operation. The degradation products were not completely removed by resin treatment. Hence, further studies in improving the efficiency of this process to eliminate the degraded products are in progress. Figure 4 shows solvent treatment setup for the studies.

Stripping the Loaded Organic using Uranous

The loaded solvent after extraction could be easily stripped with uranous ions. Crud was not observed during this operation. Hence, this can be an alternate method for reusing the spent solvent.

The diluent degraded products were responsible for the formation of surfactants and complexants which resulted in forming crud in the low acid region during stripping operation. Alkaline washes were insufficient for their removal. Adsorption of these degraded products could not be completely removed. Nevertheless, the studies will have to be continued to improve the process and extend its possibilities. Figure 5 depicts the crud formed in the set-up during mixer-settler runs.

*Reported by
A. L. Lavanya and Colleagues
Reprocessing Group*

Young Researcher's FORUM

Evaluation of Coating Thickness and Debond in Thermal Barrier Coatings using Pulsed Thermography

Coatings are widely used for protecting the structural materials from hazardous and corrosive environment by improving their surface properties. Ceramic coatings, popularly known as Thermal Barrier Coatings (TBC), are widely used for protecting the structural materials from high temperature and corrosive environment. TBCs have high temperature stability, high mechanical strength, high hardness and high chemical and erosion resistance properties. The inspection of coatings for thickness measurement, uniformity of deposition of coating and debond detection is important before using them in field. During service if the coating thickness is not up to the desired level and if the coating to substrate adhesion is not good it will lead to the premature failure of the system. Non Destructive Evaluation (NDE) methods are promising tools for coating thickness and debond evaluation due to their ability to inspect a material without impairing its future usefulness. Infrared Thermography (IRT) is one of the advanced NDE techniques which gives full field image in non contact manner with short inspection time. Pulsed Thermography (PT) is one of the popular active IRT techniques used for material and defect characterization where a short pulse of stimulus is impinged on the testing material and the signals are analyzed in transient regime. This article is focused on the feasibility study of pulsed thermography for thickness and debond evaluation in yttria coating deposited over High density graphite (HDG) substrate for pyrochemical reprocessing applications.

The coating-substrate interface is a region of thermal mismatch. The extent of thermal mismatch is given by Reflection Coefficient

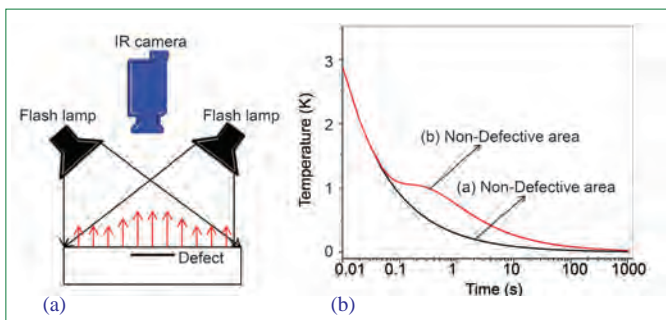


Figure 1: (a) Schematic diagram of experimental setup and (b) typical temperature decay curve



Dr. D. Sharath did his M. Sc. in Materials Science from Mangalore University in 2008 and obtained his Ph. D. from Homi Bhabha National Institute, Mumbai in 2015. He joined QAD/HSEG as Research Associate in July 2014. His areas of interest are material and defect characterization using pulsed and lock-in thermography techniques, signal and image processing.

which is defined as $R = \frac{e_1 - e_2}{e_1 + e_2}$ where e_1 and e_2 are the effusivity of coating and substrate respectively and effusivity $e = \sqrt{k\rho c_p}$ where k is thermal conductivity, ρ is density and c_p is specific heat. The value of R ranges from +1 to -1 where +1 corresponds to a perfectly reflecting interface, -1 corresponds to a perfectly absorbing interface and 0 corresponds to an interface with no thermal mismatch. In pulsed thermography, a short and high energy light pulse is impinged on the sample's surface as shown in Figure 1a. The surface absorbs the light energy and its temperature increases instantaneously. Thermal front propagates inside the material by diffusion, causing decrease in surface temperature. When thermal wave front interacts with the interface it gets reflected or absorbed causing modification in surface temperature, as shown in Figure 1b, which is monitored using IR camera. The surface temperature will increase for reflecting interface (+R) while it will decrease for absorbing interface (-R). The deviation time is a function of interface depth (thickness) and thermal diffusivity (α). This deviation time (t_p) is measured experimentally by plotting time-temperature response in logarithmic domain and computing the 1st derivative of it. If the thermal diffusivity is known then thickness (L) could be measured or vice-versa using the following equation.

$$t_p = \frac{0.693L^2}{\alpha} \quad (1)$$

The HDG and yttria coated HDG samples were received from CSTD, IGCAR for thickness measurement and coating failure characterization by Thermography. Three samples of plain HDG disc (25 mm Dia and 10 mm thick) (S1), HDG disc with SiC

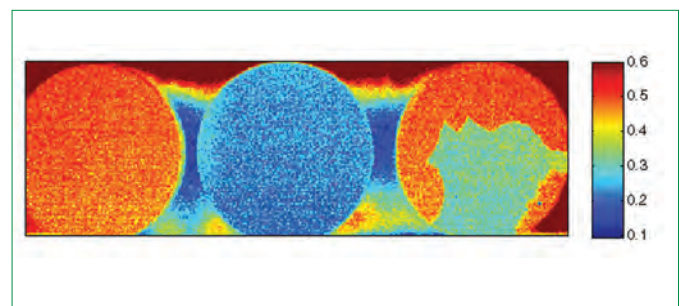


Figure 2: Thermograms of samples after 1.5 seconds of flash (a) S1, (b) S2 and (c) S3 (unit of scale is °C)

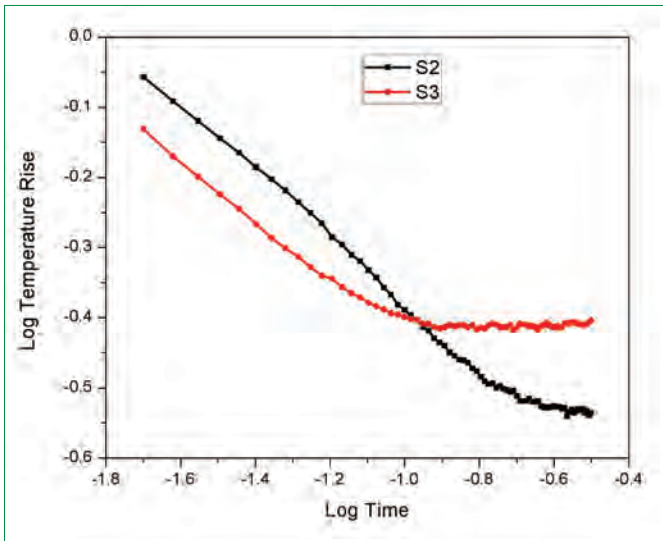


Figure 3: Temperature decay plot in logarithmic domain for samples S2 and S3

bond coat and 250-300 μm thick Yttria top coat (S2) and Coating debonded Yttria coated HDG disc after thermal cycling test at 1400 °C (S3) (as shown in Figure 2) were received for thickness and debond evaluation. The SiC coating was deposited by chemical vapor deposition and the top Yttria coating was deposited by atmospheric plasma spray process.

The values of R for SiC-HDG interface and Yttria-HDG interface were 0.1 and -0.49 respectively. Since the SiC-HDG interface had very low R and the thickness of bond coat was few tens of microns, it was difficult to measure the thickness using the available experimental set up for pulsed thermography. Whereas Yttria-HDG interface had good thermal mismatch with higher coating thickness which made the thickness measurement possible.

Experimental Details: A focal plane array based IR camera with thermal sensitivity of 25 mK and maximum frame rate of 176 Hz was used for the experiment. The detector used was Indium Antimonide with spectral sensitivity in the range 3 - 5 μm . For PT, 2 Xenon flash lamps of power 1600 W were used with pulse duration of about 3 milliseconds. Images were acquired with frame rate of 250 Hz for 15 seconds. ALTAIR software was used for acquiring and analyzing the images. The camera to object distance was kept at 25 cm.

Thermogram of the samples after 1.5 seconds of flash is shown in Figure 3. The thermogram clearly showed the temperature difference between S2 and S3. The temperature response was measured at the center of the sample and the corresponding time-temperature plot in logarithmic domain is shown in Figure 3. Since Yttria-HDG has absorbing interface ($R = -0.49$), a drop in temperature was observed when thermal front reached the interface while debonded sample registered higher temperature

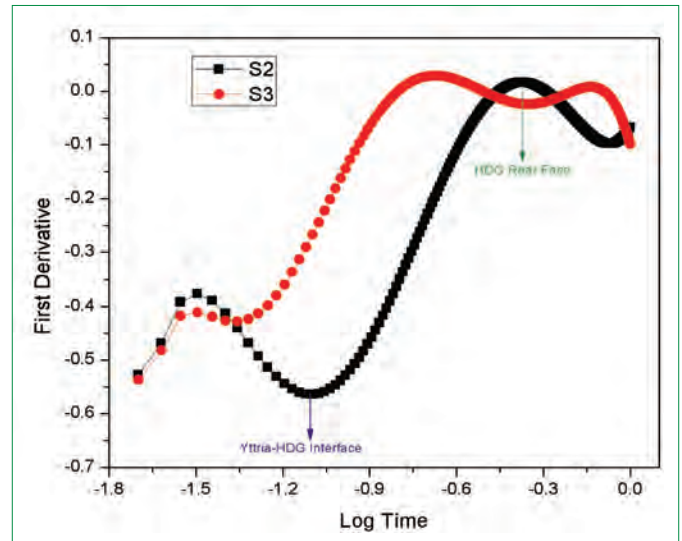


Figure 4: 1st derivative plot of sample S2 and S3

since the air gap beneath the coating (induced due to debonding) acted as barrier for the diffusion of thermal front resulting in reflecting interface as shown in Figure 3. Figure 4 shows the 1st derivative plot as a function of log time for samples S2 and S3. For S2, initially a trough and finally a crest were observed. The trough corresponds to the Yttria-HDG interface while the crest corresponds to HDG-Air interface at the rear surface. The value of thermal diffusivity of Yttria considered for thickness measurement was 1.25 mm^2/s (experimentally measured). The 1st derivative peak time was measured and the coating thickness was obtained using equation (1). The measured thickness was 396 μm which is in good agreement with the thickness of 380 μm obtained from Eddy current/Hall effect thickness gauge measurements. It is inferred from Figure 4 that the sample S3 did not show a trough but it showed a diffused crest at intermediate stage indicating complete delamination of coating. Hence, from the thermograms as well as from the 1st derivative plot, well bonded coatings can be clearly differentiated from debonded coatings. The initiation of debond could be predicted at early stage when the peak starts to shift from its usual trend.

The present study showed the capability of pulsed thermography for thickness and debond evaluation in ceramic coatings. Coating thickness was successfully measured in Yttria-HDG coating system with 4.2% error and the debonded area could be clearly detected in the coating system. Future study would be focused on predicting the debond initiation at the early stage.

*Reported by
D. Sharath and Colleagues
Health, Safety & Environment Group*

Visit of Dignitaries



Delegations from United States Nuclear Regulatory Commission led by Dr. Stephen Burns with Dr. A.K. Bhaduri, Director, IGCAR and senior colleagues of the Centre

A delegation from United States Nuclear Regulatory Commission led by Dr. Stephen Burns, Chairman, US Nuclear Regulatory Commission visited the Centre on November 9, 2016. The delegation visited the Fast Breeder Test Reactor, KAMINI, Radio Metallurgy Laboratory, facilities in Fast Reactor Technology Group and Reactor Design Group.



Prof. A. K. Bhowmik, Professor of Eminence, RTC, IIT Kharagpur during the IGC Colloquium

Prof. A. K. Bhowmik, Professor of Eminence, RTC, IIT Kharagpur and former Director, IIT, Patna delivered IGC Colloquium on the topic “Nanotechnology in the Field of Polymers” on November 11, 2016



Prof. Vijayamohan K Pillai, Director, CECRI delivering the IGC Colloquium

Prof. Vijayamohan K Pillai, Director, Central Electrochemical Research Institute delivered IGC Colloquium on the topic “Large-scale Energy Storage using Redox Flow Batteries” on November 23, 2016

Visit of Dignitaries



Dr. Srikumar Banerjee, Homi Bhabha Chair Professor, DAE & Former Chairman, AEC during the IGC Colloquium

Dr. Srikumar Banerjee, Homi Bhabha Chair Professor, DAE & Former Chairman, AEC delivered IGC Colloquium on the topic "Nuclear Power from Thorium - Different Options" on November 29, 2016

Forthcoming Meetings / Conferences

An International Conference on Electron Microscopy and Allied Techniques (EMSI 2017)

July 17–19, 2017

The International Conference on Electron Microscopy and Allied Techniques during July 17–19, 2017 at Confluence Banquets and Resort, Mamallapuram will be jointly organized by Indra Gandhi Centre for Atomic Research, Kalpakkam and the Indian Institute of Technology Madras, Chennai under the aegis of Electron Microscope Society of India (EMSI). EMSI - 2017 includes a wide range of topics from Materials Science to Life Sciences. Dedicated sessions will include discussions on advances in SEM, TEM and other complementary and emerging techniques such as Atom Probe Tomography, Fluorescence. Microscopy, SPM, STM, Confocal Microscopy, AFM etc. The scope of the conference includes but is not restricted to

Advanced Microscopy Techniques: Aberration Corrected TEM & STEM, SEM – FIB, Ion Beam Microscopy, Electron Diffraction & Crystallography, SPM, HREM, OIM, In-situ and Environmental Microscopy, Microscopy based microanalysis, Cryo Electron Microscopy, 3D-APT, etc.

Application of Microscopy to Novel Materials: Functional Materials, Plasmonics, Thin films and Coatings, Low dimensional Materials, Aperiodic structures, Electronic Materials, Nanomechanics etc. Engineering Materials including behavior under extreme environments.

Bio Nanotechnology Medical Applications: Imaging host – pathogen interaction, brain structure, virology, immuno-electron microscopy and microanalysis Biological Sciences: Application in palaeontology and palaeobiology, flow cytometry and in vivo imaging Geological Materials: Earth and Planetary Materials, Sedimentary and associated rocks, climate research.

Address for Correspondence:

Dr. Arup Dasgupta
Convener, EMSI – 2017
Head, Structural and Analytical Microscopy Section,
Physical Metallurgy Division, Metallurgy and Materials Group,
Indira Gandhi Centre for Atomic Research, Kalpakkam, TamilNadu, India.
Phone: +91 44 2748 0202; Fax: +91 44 2748 0202;
Mob. (8PM - 8AM IST): +91 94449 65532
E-Mail: emsi2017@igcar.gov.in, arup@igcar.gov.in
website: <http://emsi.org.in/emsi2017/>

Submission of Abstracts:

February 23, 2017

Closing of Abstract Submission:

April 15, 2017

Intimation of Acceptance of Abstracts:

May 15, 2017

DAE Awards

Department of Atomic Energy has instituted annual awards for excellence in Science, Engineering and Technology in order to identify best performers in the area of Research, Technology Development and Engineering in the constituent units (other than Public Sector Undertakings and Aided Institutions). The Young Applied Scientist, Young Engineer, Young Technologist, Homi Bhabha Science and Technology Award and Scientific and Technical Excellence Award fall under this category. Group Achievement awards for recognition of major achievements by groups have also been instituted. Life-time Achievement Award is awarded to one who has made significant impact on the DAE's programmes. They are the icons for young scientists and engineers to emulate. The awards consist of a memento, citation and cash prize.

The recipients of the Awards from IGCAR for the year 2015 are:

Homi Bhabha Science and Technology Award	: Dr. John Philip, MMG
Scientific and Technical Excellence Award	: Dr. Divakar Ramachandran, MMG Dr. Anish Kumar, MMG
Young Applied Scientist / Technologist Award	: Shri Ranga Ramakrishna, FRTG Shri T. K. Haneef, MMG
Young Engineer Award	: Shri T. Sakthivel, MMG Shri Piyush Kumar Aggarwal, FRTG Shri Ram Kumar Maity, RDG Shri R. Dheenadhayalan, EIG
Meritorious Technical Support Award	: Shri M. Rajendran, RFG Shri A. Amalraj, MC&MFCG Shri K. Kamaludeen, RFG
Meritorious Service Award	: Shri A. Christopher, Administration Shri Sairam Ramadorai, Director's Office

Group Achievement Awards:

Development of Nitrogen Enhanced 316LN Austenitic Stainless Steel for Primary Components of Sodium Cooled Fast Reactors.

Dr. A. K. Bhaduri, Director, IGCAR, Group Leader

Dr. U. Kamchi Mudali, Dr. K. Bhanu Sankara Rao, Dr. M. D. Mathew, Dr. K. Laha, Dr. Shaju K. Albert, Dr. B. K. Choudhary, Dr. C. Mallika, Dr. N. Parvathavarthini, Dr. R. Sandhya, Dr. P. Parameswaran, Dr. V. S. Srinivasan, Dr. M. G. Pujar, Dr. A. Nagesha, Dr. S. Ningshen, Shri G. Srinivasan, Dr. S. Ravi, Dr. Vani Shankar, Dr. G. V. Prasad Reddy, Shri J. Ganesh Kumar, Shri M. Nandagopal, Dr. Sunil Goyal, Shri J. Christopher, Ms. P. Poonguzhuli, Dr. Anita Topoo, Shri V. David Vijayanand, Shri T. Sakthivel, Shri R. Kannan, Shri Aritra Sarkar, Shri Durga Prasad Rao Palaparti, Ms. M. Divya, Shri K. Thyagarajan, Shri N. Sivaibharasi, Shri V. Ganesan, Shri Srinivas Manneppalli, Shri K. Mariappan, Ms. S. Panneerselvi, Shri A. Vinod Kumar, Shri N. S. Thampi, Shri K. Vaithiyathan, Shri S. Sakthy, Shri M. Arul, Shri M. Gandhi, Shri M. Srinivasarao, Shri M. Munivel, Ms. R. Uma Maheswari, Ms. M. Jayalakshmi, Shri M. Govindaswamy, Ms. Indira Logu, Ms. M. Esakkiammal and Ms. N. Santhi from **MMG**

Remote Replacement of Radiation Shielding Window and resolution of Challenges during Operation at CORAL Facility

Dr. A. Ravishankar, RpG & Shri V. Vijayakumar, RpG - Group Leaders

Shri K.C. Ajoy, Shri A. Dhasekaran, Dr. B. Venkataraman, Dr. M.T. Jose, Shri V. Rajagopal, Shri R. Santhanam, Shri S. Viswanathan, Shri R. Mathiyarasu, Shri S. Baskar, Dr. S. Kalaiselvan, Shri S. Chandrasekaran, Dr. U. Madhusoodanan, Shri S. Balasundar, Dr. O. Annalakshmi, Dr. M. Manohari, Shri R. Arul, Ms. R. Akila, Shri S.M.S Murthy, Shri D. Karthikeyan, Shri N. Yuvaraj and Ms. Nitu Sinha from HSEG; Shri B. M. Ananda Rao, Shri E. Balu, Shri A. Palanivel, Shri G. Surendar Kumar, Shri Apurba Kumar Majumder, Shri MD. Mohaiddain Ansari, Shri K.K. Shimjith, Shri N. Divakar, Shri M. Elumalai, Shri K. Ajai Kumar, Shri S.S. Kumar Goru, Shri C. Kannan, Shri V. Venugopal, Shri N. Govindan, Shri G. Rajendran, Shri Prashant Kumar, Shri M. Dhayalan, Shri T. Sengalani, Shri S. Sengayani, Shri L.A. Leo Felix, Shri H. Humayoun, Shri Shekar Kumar, Shri Surajit Halder, Shri M. Muthukumar, Shri Kinkar Mandal, Shri Peeyush Gupta, Shri Varatharajan, Shri J. Thiyaga Senthilkumar, Shri S. Somasundaram, Shri Sajju George, Shri S. Sivakumar, Shri Abdul Muqtadir, Shri M. Selvarasan, Shri R. Sajikumar, Ms. Radha Rani, Shri Vijayaraghavan, Shri K. Arasakumar, Shri D. Natarajan, Shri K. Ilanchezhian, Shri Ravi Islavath, Shri N. Balasubramanian, Shri Potta Ramjee, Shri P. Santhanadevan, Shri V. Kumara Vijayan, Shri M. Suresh, Shri A.K. Sasi, Shri S. Pandurangan, Shri P. Ramesh Kumar, Shri K.K. Vinod Kumar, Ms. C.M. Bagyalakshmi, Shri L. Yogananth, Shri J. Madhusudhana Rao, Shri M. Bhaskar, Shri Ashish Shriram Ladhe, Shri Nanhe Rajendra Manohar, Shri Harendra Kumar, Shri J. Palanivel, Shri Ramprasad Pal, Shri Ghanshyam Kumar, Shri N. Sreekumar, Shri Bonu Sanyasi Rao, Ms. N. Abirami, Shri E. Krishnamurthy, Shri M. Ananthan, Dr. R. V. Subba Rao, Dr. P. Govindhan, Shri K. Dhamodharan, Shri D. Jebaraj Mahildoss, Dr. P. Sivakumar, Dr. S. Sukumar, Shri K.S. Vijayan, Shri D. Sivakumar, Shri G. Santhosh Kumar, Shri S. Parthasarathy, Dr. M. Subha, Shri S. Ganesh, Shri Pradeep Kumar Sharma, Shri S. Pugazhendi, Shri S. Sudhagar, Shri T. Aneesh, Shri Satya Narayan Das, Shri Saptarshi Chatterjee, Shri Akhilesh K. Nair, Ms. K. Ponkamini Sasirekha, Ms. C.S. Suganya Devi, Shri K. Stanley, Shri R. Karthick, Shri Shantaram Jandhyala, Shri I. Sriharsha, Ms. D. Jayanthi, Shri K. Rajkumar, Shri S. Prakash, Ms. T. Selvi, Ms. C. Shibina, Ms. V. Varalakshmi, Ms. S. Poongudi, Ms. Bhavya S. Nair, Shri Suresh Borado, Shri A. John Deepak Lawrence, Ms. G. Preetha, Shri Saurabh Suman, Shri V. Anandha Narayanan, Shri N. Srinivasan, Shri Aravind Kumar Meena, Shri Alok Kumar Mishra, Shri B. Krishnamurthy, Shri Geo Mathews, Shri M. S. Gopikrishna, Shri P. Vijayasekaran, Shri R. Amudhu Ramesh Kumar, Shri J. W. Reuben Daniel, Shri R. N. Verma, Ms. Swatilekha Bhattacharjee, Ms. M. Swapna, Shri Padi Srinivas Reddy, Shri S. Manickam, Shri P. C. Sandheep, Shri. K. P. Desheeb, Shri M. Vinoth Kumar, Shri P. Anbazhagan, Shri R. Anbarasan, Ms. B. Uma, Ms. P. G. Sethulakshmi, Shri G. Alagesan, Shri C. U. Jayakumar, Ms. G. Maheswari, Shri. D.C. Thomson, Shri S. Pushpa Selva Kumar, Shri Pradip Paul, Shri R. Gopalakrishnan, Shri C. Murugesan, Shri S. Ramesh, Shri P. Sudalaimani, Shri G. Velu, Shri A. K. Kannan, Shri S. Suresh Babu, Shri R. Mouli, Shri K. Paramasivan, Shri K.G. Ramesh Babu, Shri E. Murthy, Shri A. Jahangeer, Shri M. V. Praveen Kumar, Shri A. Vilvanathan, Shri S. Venkatesh, Shri Satish Verma, Shri K. Damodaran, Shri V. Raja, Shri Satish Kumar Velaga, Shri V. Muralikrishnan, Shri R. Ganesan, Shri K. Sampath, Dr. C. Mallika, Shri K. Rajan, Shri N. K. Pandey, Shri N. Krishnan, Shri R. Rajeev, Ms. Heera Balachandran, Dr. Falix Lawrence, Shri Jayendra Kumar D. Gelatar, Shri B. Lokeshwara Rao and Shri T. Dinesh from RpG

Testing and Qualification of HTFC in FBTR & KAMINI

Shri C. P. Nagaraj, EIG, Group Leader

Shri C. P. Nagaraj, Shri K. Madhusoodanan, Shri M. Sivaramakrishna, Shri Chandrakant Upadhyay, Shri N. Anand Kumar, from EIG. Shri G. Srinivasan, Shri K. V. Suresh Kumar, Shri S. Varatharajan, Shri A. Babu, Shri S. Sridhar, Shri G. Shanmugam, Shri K. Bhanumurthy, Shri T.V. Ravindranath, Shri M. Murugesan, Shri A. Mani, Shri K. Asokan, Shri B. Kadirappa, Ms. P. Akilandeswari, Shri Dinkar Jha, Shri B. Manoharan, Shri P. Saravanan, Shri K. G. Subramanian, Shri S. Kanagaraju, Shri K. Kamaludeen, Shri D. Vinoth, Shri V. Velu, Shri M. Jayasankar, Shri V. Rajkumar, Shri D. Jaisrinivasan, Shri A. Udaya Shankar, Shri V. Padmanaban, Shri B. Dharmiah, Shri M. Babu, Shri D. Vignesh Babu, Shri N. Kathresan, Shri M. Arumugam, Shri R. Gopal, Shri P. Maharajan, Shri C. Kannan, Shri R. Sekar, Shri N. Manimaran, Shri N. Balakrishnan, Shri D. Visweswaran, Shri M. Elumalai, Shri J. V. Srinivasan, Ms. Sheela Nambiar, Shri M. Elango, Shri J. Sasi Kumar, Dr. S. Sivakumar, Shri G. Raghukumar, Ms. E. Radha, Shri V. Sathiamoorthy from RFG; Shri V. Praveen Kumar, Shri Karuppasami, Shri S. Murugan, Shri D. Dileep, Shri V. Kodiarasan, Shri S. Yuvaraj, Shri E. Gothandan, Shri B. Ramalingam, Shri P. Shunmugam from ESG; Shri P. Ramesh, Shri Uma Shankar and Shri B. Govindaswamy from HSEG
Shri K. Natesan from RDG



Awards and Honours



Dr. M. Sai Saba, Director, RMG has been elected as an “Executive Member” for the Academy of Sciences, University of Madras, Chennai

Dr. G. K. Sharma, Non-Destructive Evaluation Division, MMG, received “Dr. T. K. Saksena Memorial Award” for the best Ph. D. thesis titled “Ultrasonic NDE of Type 316 Austenitic Steel by Time Frequency Analysis” by Ultrasonics Society of India

Dr. M. Vasudevan, Materials Technology Division, MMG has been awarded “Metallurgist of the Year Award 2016” by the Steel Ministry Government of India during 54th National Metallurgist Day Awards at Indian Institute of Technology, Kanpur on November 14, 2016



Best Paper/Poster Award



Setting up of Holographic Optical Tweezer Arrays

Shri Deepak K. Gupta

61st DAE Solid State Physics Symposium, Board of Research in Nuclear Sciences, DAE, December 30, 2016

Best Poster Award

High Temperature Mass Spectrometric Studies on U-19Pu-6Zr

Shri P. Manikandan, Shri V. V. Trinadh, Shri M. Prasad, Dr. T. S. Lakshmi Narasimhan, Dr. M. Joseph

6th Interdisciplinary Symposium on Materials Chemistry (ISMC-2016) at BARC, Mumbai, December 6-10, 2016

Best Paper Award

Experimental Determination of Liquidus of Fe-Zr by Spot Technique

Shri P. Ramakrishna, Shri B. Samanta, Shri S. Balakrishnan, Dr. K. Ananthasivan

6th Interdisciplinary Symposium on Materials Chemistry (ISMC-2016) at BARC, Mumbai, December 6-10, 2016

Best Paper Award



Lanea coromandelica or Indian Ash Tree

Dr. M. Sai Baba,

Chairman, Editorial Committee, IGC Newsletter

Editorial Committee Members: Shri M. S. Chandrasekar, Dr. N. V. Chandra Shekar, Dr. T. S. Lakshmi Narasimhan
Dr. C. Mallika, Shri V. Rajendran, Dr. Saroja Saibaba, Dr. C. V. Srinivas and Dr. Vidya Sundararajan